Effect of Buffer Layer selection on Perovskite-Based Solar Cell Efficiency: A Simulation Study Using OghmaNano Software

B Mourched[1]*, S Sawaya[2], M Abdallah[3], N Abboud[2]

1. College of Engineering and Technology, American University of the Middle East, Egaila 54200, Kuwait

2. Faculty of Science II, Lebanese University, Lebanon

3. Faculty of Science III, Lebanese University, Lebanon

ABSTRACT

This simulation paper investigates the impact of incorporating three different buffer layers (CZTSE, CZTS, and CZS) on the efficiency of two different types of perovskite absorber layers ($MAPbCl_3$ and $MAGeI_3$) in a solar cell using the OghmaNano software. The absorber thickness is optimized for maximum efficiency, and then each type of buffer layer is optimized for further efficiency gains. Results show that $MAGeI_3$ has higher efficiency values compared to $MAPbCl_3$. Moreover, the CZS buffer layer demonstrates a remarkable increase in efficiency compared to CZTS and CZTSe buffer layers, with a difference of up to 23.35% for $MAPbCl_3$ and 6.8% for $MAGeI_3$. This study highlights the importance of buffer layer selection and optimization for achieving higher solar cell efficiency.

1. INTRODUCTION

Hybrid perovskite solar cells have made a significant impact in the field of photovoltaics, with their efficiency rapidly increasing from 4% to 26% in a short period of time [1], while it took over 40 years for other materials to see the same level of improvement [2]. The structure of lead hybrid perovskites is based on the $MAPbX_3$ formula, where MA is an organic or inorganic cation and X is a halide. Their exceptional optoelectronic properties, such as a high optical absorption coefficient [3], low trap density [4], and shallow defect states, contribute to their high performance. Additionally, the simplicity of processing these materials from solutions at or near room temperature in just a few months, as compared to the several years required for silicon solar panels [5], makes them a promising option for the future of photovoltaics and solar energy.

Hybrid perovskite materials, such as $CH_3NH_3PbCl_3$, have gained significant attention in recent years due to their exceptional properties, including high absorption of ultraviolet and visible light, adjustable band gaps, and long electron-hole diffusion lengths [6]. These metal halide perovskites are low-cost and can be processed from solutions, making them suitable for future technologies. However, the stability of these materials in the presence of heat, oxygen, moisture and other environmental factors [7] and the presence of the toxic element lead (Pb) have been identified as major obstacles to their large-scale fabrication. In order to find suitable substitute elements, researchers have suggested looking at elements that have similar chemical and physical properties to lead, such as Bi, Ge, Sb, In, Ag, Te, and Sn [8].

*Corresponding Author: bachar.mourched@aum.edu.kw

Studies have indicated that perovskite materials based on Germanium (Ge) may offer a feasible alternative to the traditional lead-based materials used in solar cells. $CH_3NH_3GeI_3$, a hybrid organic-inorganic germanium perovskite, boasts adjustable bandgap and can be synthesized with ease through solution processing [9]. Furthermore, this material has demonstrated superior optical and electronic properties, improved electron and hole behavior, and superior hole behavior when compared to $CH_3NH_3PbI_3$ [10-12]. Another advantage of Ge is its ability to maintain stability even at elevated temperatures up to 150°C, making it a more favorable option for PSC device fabrication [13]. These qualities suggest that the use of germanium-based perovskite solar cells could lead to more efficient and environmentally friendly outcomes in the future.

This paper utilizes OghmaNano (Organic and hybrid Material Nano), a simulation tool for modeling various photovoltaic devices, including organic and inorganic photovoltaics and dye-sensitized solar cells. It is a powerful tool for researchers and engineers working in the field of solar cell technology as it uses a detailed physical model to simulate the transport of charge carriers in the solar cell, considering factors such as recombination, carrier mobility, and trap-assisted recombination [14-16].

The focus of this study is on two perovskite materials defined as absorber layers in the simulation- platform. The objective is to model, analyze, and optimize the photovoltaic device structure and examine output parameters such as open circuit voltage (V_{oc}), current density (J_{sc}), fill factor (FF), and efficiency.

The paper has two primary objectives. Firstly, it aims to compare the power conversion efficiency (PCE) of two distinct perovskite solar cell structures ($MAPBCl_3$ and $MAGeI_3$). Secondly, it seeks to examine the impact and significance of incorporating buffer layers in solar cells on their power conversion efficiency. To accomplish this, various parameters are investigated and optimized to achieve the highest possible efficiency.

The proper selection of the absorber and carrier transport layers and their thicknesses, namely the electron transport layer (ETL) and hole transport layer (HTL), is vital for improving the efficiency of the device. Thus, the best combination of both the ETLs and HTLs is to be sustained for improvement in device efficiency [17].

The Hole Transport Layer (HTL) enables efficient hole transport from the photogenerated layer to the electrodes. The properties of the HTL material, such as its electrical conductivity, hole mobility, and charge recombination rate determine the solar cell performance [18,19]. Different materials have been proposed as HTLs in organic, inorganic or hybrid solar cells such as Spiro-OMeTAD, Poly(3,4-ethylenedioxythiophene) (PEDOT), copper phthalocyanine (CuPc) and molybdenum oxide (MoOx), and others [20,21]. Cu_2O is also used as HTL due to its unique properties that make it a promising material for photovoltaic applications such like its high absorption coefficient, high electrical conductivity, high stability under long time light irradiation [22,23].

The electron transport layer (ETL) material is responsible for collecting and transporting electrons generated by the absorption of photons in the solar cell to the electrodes, and its choice has a significant impact on the performance of the cell. The hybrid perovskite ETL material has gained significant interest due to its enhanced electron mobility and adjustable bandgap, which results in improved light absorption and elevated power conversion efficiency in solar cells [24-26]. TiO_2 was used as an ETL in lead-based perovskite solar cells, as referenced in [27], resulting in a high PCE of 17.46%. However, TiO_2 has limitations as an

ETL because of its low carrier mobility and negative effects on device stability under UV light [28,29]. Other materials used in solar cells include Copper Indium Gallium Selenide (CIGS) [30], Cadmium Telluride (CdTe) [31], Perylene Diimide (PDI) [32], Non-fullerene Acceptors (NFAs) [33], and P3HT:PCBM [34]. SnO_2 is also well-suited for use as an ETL layer because of its wide bandgap, which ensures that it does not absorb light and reduces recombination losses. Additionally, it has a high electron mobility, a high transparency in the visible region, a low cost and stability under operating conditions, and a wide range of workability making it easy to deposit and process. Many research works highlighted the importance of the SnO_2 material as ETL in improving the solar cell efficiency [35-39].

2. BUFFER LAYER IMPORTANCE

The buffer layer, lying between the absorber layer and the electrode, plays a critical role in improving the efficiency and stability of the solar cell, making it an important component in the design and construction of high-performance solar cells. The primary function of the buffer layer is to reduce the recombination of the charge carriers (electrons and holes) that are generated when the light strikes the absorber layer presenting a barrier between the absorber layer and the electrode. It also improves the adhesion of the absorber layer to the electrode and reduces the likelihood of the formation of shunt paths in the solar cell. Additionally, the buffer layer can also modify the energy band alignment between the absorber layer and the electrode, which can further enhance the performance of the solar cell and improve the efficiency of charge transfer at the interface. The selection of the buffer layer material depends on various factors such as the type of absorber material used, the fabrication process, and the desired performance characteristics of the solar cell. Several materials are commonly used as buffer layers and utilized in the production of thin films and nanostructured materials for photovoltaic devices, such as Cadmium sulfide (CdS), Zinc oxide (ZnO), copper zinc tin sulfide (CZTS), Copper Zinc Tin Selenide (CZTSe), cadmium telluride (CdTe), dye-sensitized solar cells (DSSCs), copper indium disulfide ($CuInS_2$) and others [40-44]. At present, the primary challenges for the advancement of thin film solar cells are to decrease manufacturing costs while also increasing efficiency and performance.

With its low cost, non-toxic, suitable bandgap of about 1.6 eV, high absorption coefficient of visible light (above 104 cm^{-1}), and its widely available constituent elements, CuZnS (CZS) is a favorable option for creating thin film solar cells due to its appropriate optical and electrical characteristics. It is a promising material which can serve as a cost-effective substitute for $CuInS_2$ and CZTS. CZS is an alloy material composed of Cu_xS and ZnS, where the expensive indium in the material is replaced by cheaper and more abundant Zn. CZS demonstrates a double band gap due to its alloy nature, with the lower band gap being useful for absorbing light, and the higher band gap serving as a window layer for solar cells. CZS has been applied in Inorganic Electroluminescence applications [45] and can be prepared through various techniques such as pulsed laser deposition [46], chemical bath deposition [47], electrochemical deposition [48], and photochemical deposition. Reference [49] reported that the electrical conductivity of CuZnS thin films prepared by Chemical Spray Pyrolysis, can be increased by 4 orders by just increasing the Cu concentration which also leads to decrease of band gap from 3.4 eV to 1.8 eV. Other work reported a maximum electrical conductivity of 7.38×10^{-2} (Ω.cm)-1 and minimum electrical resistivity of 1.35 (Ω.cm) obtained for a (CZS) film deposited at 470 ^{O}C, with high-quality CZS thin films deposit [50].

In this context, we are studying the effect of incorporating a CZS buffer layer between the absorber layer and the front contact layer on the performance of a solar cell. As the specific functions of the buffer layer is also depending on the materials being used in the solar cell, the importance of the choice of the absorber material is also highlighted in this report.

The structure of the paper is outlined as follows: the solar cell structure, the materials used and their optimum dimensions, and the simulation parameters are provided in Section 3. The section 4 presents the effect of the CZS buffer layer on the key parameters describing the solar cell performance such as the open circuit voltage (V_{oc}), the short circuit current (I_{sc}), the fill factor (FF), and the efficiency. This study is performed for two different absorbers, lead halide (CH3NH3PbCl3) and lead free (CH3NH3GeI3). The buffer layer and absorber thicknesses that yield the highest power conversion efficiency are established, and their implications are also discussed.in section 4. Section 5 concludes with an assessment of the significance of the buffer layer and material selection in solar cells.

3. STUDY DESIGN AND PARAMETERS

As aforementioned, the choice of materials and design of the carrier's transport layers has a significant impact on the device's efficiency, speed, stability, and reliability. In this report, the fluorine-doped tin oxide (FTO) is used as a transparent conducting oxide (TCO) in the front electrode of the solar cell allowing light to pass into the active layer serving as an electrical contact to the active layer. The fluorine doping in FTO improves its electrical conductivity and enhances its transparency in the visible spectrum.

The HTL material is chosen to be SnO_2 as it is known by its high transparency with a bandgap of 3.6 ev allowing a maximum light transmission to the active layer, its high electric conductivity enabling an efficient way of holes transportation, and its high work function minimizing the energy loss occurring when charge carriers move between layers in the solar cell. The ETL material is chosen to be Cu_2O as it has a conduction band energy level that is well aligned with the lowest unoccupied molecular orbital of many organic semiconductors, making it an effective ETL. The relatively low conduction band offset of Cu_2O can also result in a higher open-circuit voltage in the device. Additionally, Cu_2O has a high hole-blocking capability, which helps to minimize the recombination of electrons and holes at the interface between the ETL and the active layer. This can result in higher device efficiency.

Gold (Au) is used as back contact as it is a noble metal, meaning it is resistant to corrosion and oxidation. This makes it a good choice for a back contact material, as it will not react with other materials in the solar cell and will remain stable over time. It represents an excellent conductor of electricity, which is important for efficient collection and transport of the electrical current generated by the solar cell. Furthermore, Au is a highly reflective material, which can help to increase the amount of light that is absorbed by the solar cell.

Two perovskites' materials are proposed to define the active layer in the solar cell. Absorber 1 material is the methylammonium lead (II) chloride ($CH_3NH_3PbCl_3$ or $MAPbCl_3$) and absorber 2 material is the methylammonium germanium (IV) triiodide ($CH_3NH_3GeI_3$ or $MAGeI_3$). The importance of $MAPbCl_3$ and $MAGeI_3$ in solar cells lies in their high-power conversion efficiency, low cost, and ease of fabrication. While there are still challenges to be addressed, perovskite solar cells have the potential to revolutionize the field of photovoltaics and play a key role in the transition to a more sustainable and renewable energy future.

The structure of the simulated configuration is presented in figure 1 where the buffer layer will be introduced between the absorber layer and FTO layer.

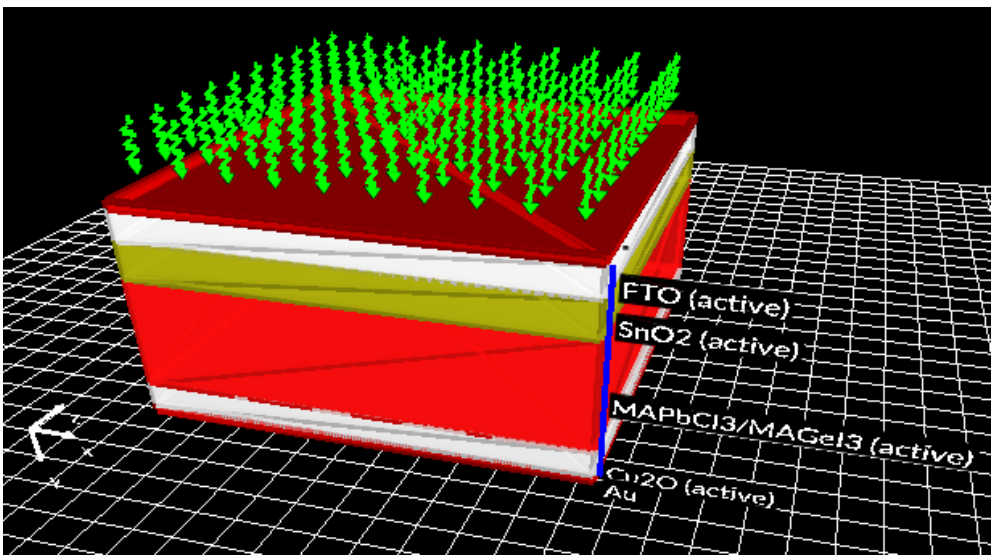

Figure 1: Solar cell structure design using OghmaNano software.

The FTO, SnO_2, Cu_2O, and Au material thicknesses providing the maximum efficiency, are set to be 200, 70, 350, and 100 nm, respectively. In the initial investigation, the objective is to identify the optimal thickness for each absorber that would yield the highest output parameters of the solar cell, including V_{oc}, I_{sc}, FF, and efficiency $\eta(\%)$. This analysis is performed in the absence of the buffer layer, with absorber thickness ranging from 200 to 900 nm at intervals of 50 nm for both absorbers. The outcomes of the solar cell output parameters are presented in figure 2.

From observing figure 2, it is apparent that absorber 2 has higher V_{OC}, J_{SC}, FF and $\eta(\%)$ values compared to absorber 1. From figure 2.a, V_{OC} values for both absorbers demonstrate an increasing trend with an increase in absorber thickness, until a thickness of 600 nm is reached, where the values stabilize. Figure 2.b illustrates that the J_{SC} values for both absorbers experience a decline until they reach a minimum value at a thickness of 600 nm, after which they increase once again. In Figure 2.c, constant FF values are observed for both absorbers. In figure 2.d, results reveal that absorber 1 reaches peak efficiency of 22.27% at a thickness of 600 nm, and absorber 2 achieves maximum efficiency of 25.58% at the same thickness. Absorber 2 outperforms absorber 1 in terms of efficiency. Consequently, 600 nm is established as the optimal thickness for both absorbers based on these findings.

It is important to mention that the studies conducted in this work have shown similar behavior patterns for V_{OC}, J_{SC} and FF. As a result, the efficiency output $\eta(\%)$ will be the only parameter presented in all forthcoming studies. The subsequent discussion focuses on the influence of including a buffer layer on the output parameters of a solar cell. This analysis uses absorbers 1 and 2 with an optimal absorber thickness of 600 nm.

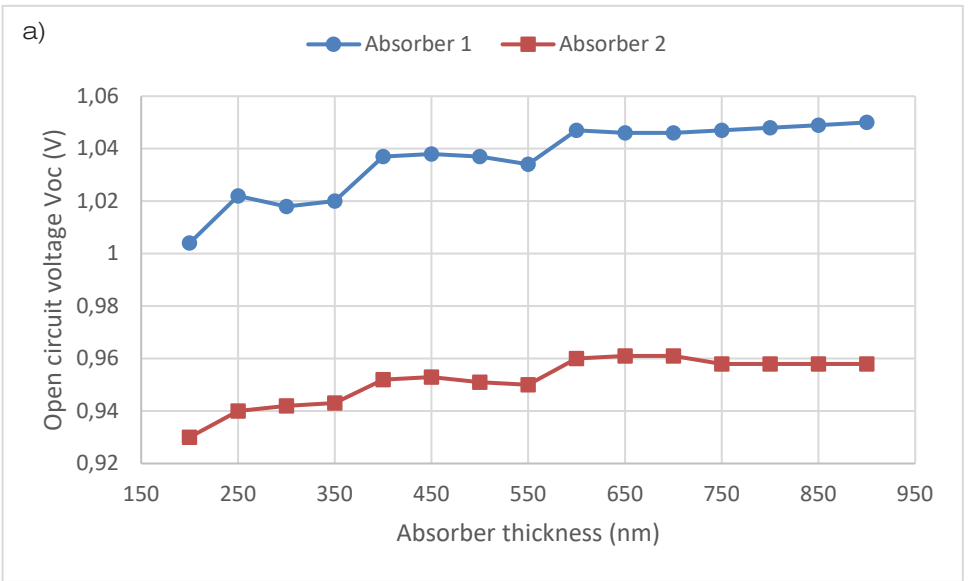
a)
Absorber 1
Absorber 2
Open circuit voltage Voc (V)
1,06
1,04
1,02
1
0,98
0,96
0,94
0,92
150
250
350
450
550
650
750
850
950
Absorber thickness (nm)

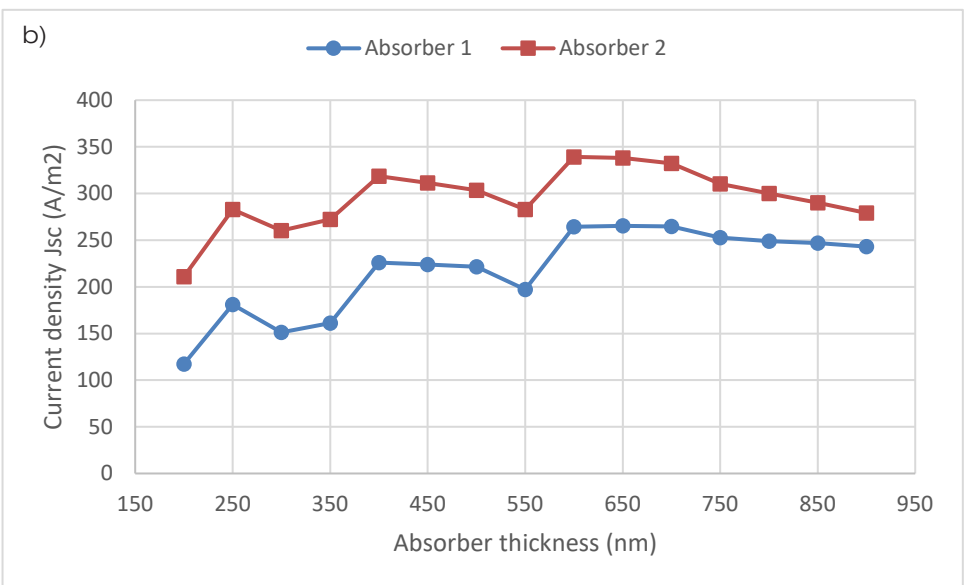
b)
Absorber 1
Absorber 2
Current density Jsc (A/m2)
400
350
300
250
200
150
100
50
0
150
250
350
450
550
650
750
850
950
Absorber thickness (nm)

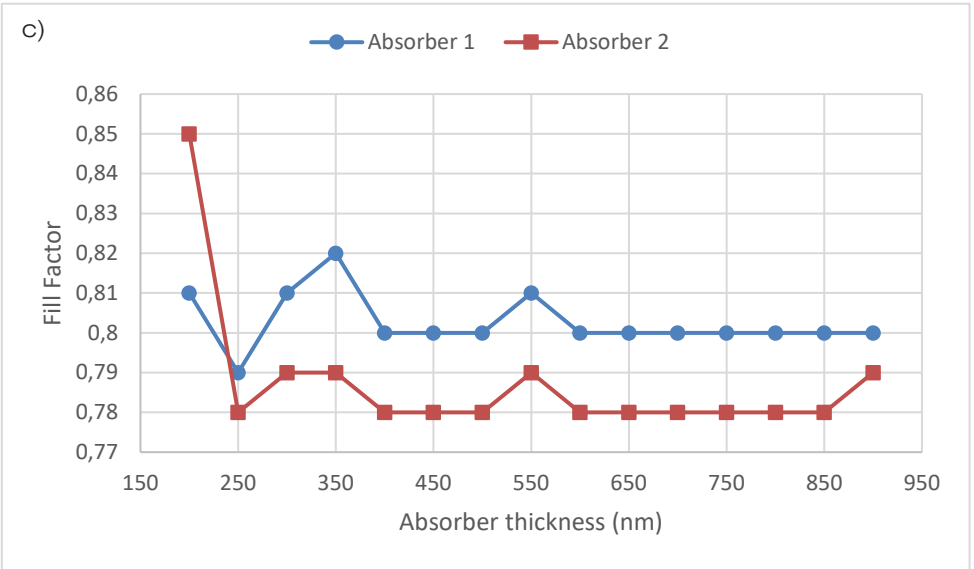

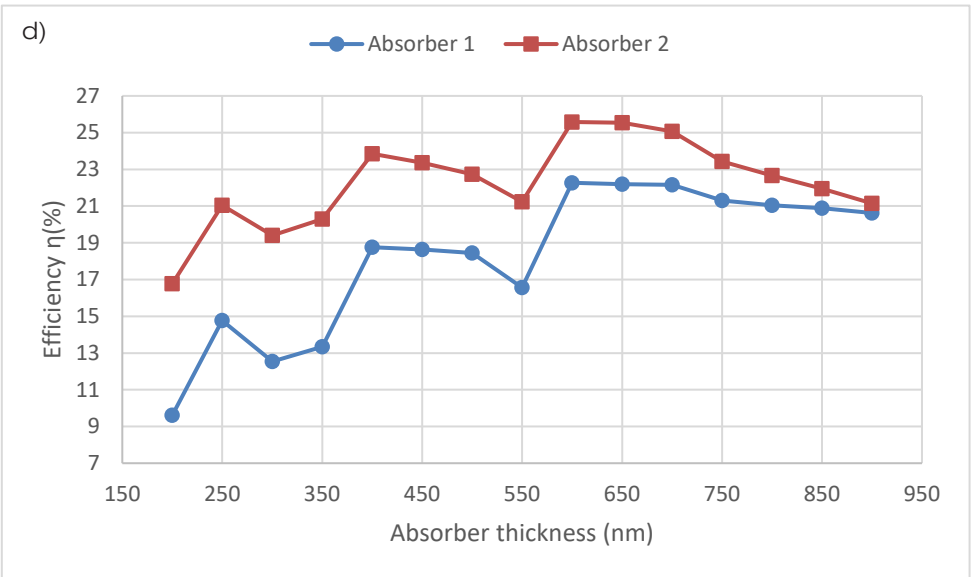

Figure 2: Solar cell output parameters in term of absorber thickness a) V_{OC}, b) J_{SC}, c)FF, d) $\eta(\%)$

4. RESULTS, ANALYSIS, AND DISCUSSION

This section presents an analysis of the power conversion efficiency of solar cells with three different types of buffer layers: CZTSe, CZTS, and CZS. By varying the thickness of the buffer layer from 50 to 500 nm in increments of 50 nm, the optimal thickness that results in the highest efficiency is determined. The solar cell efficiency for each type of buffer layer is shown in Figure 3 for CZTSe, figure 4 for CZTS, and figure 5 for CZS.

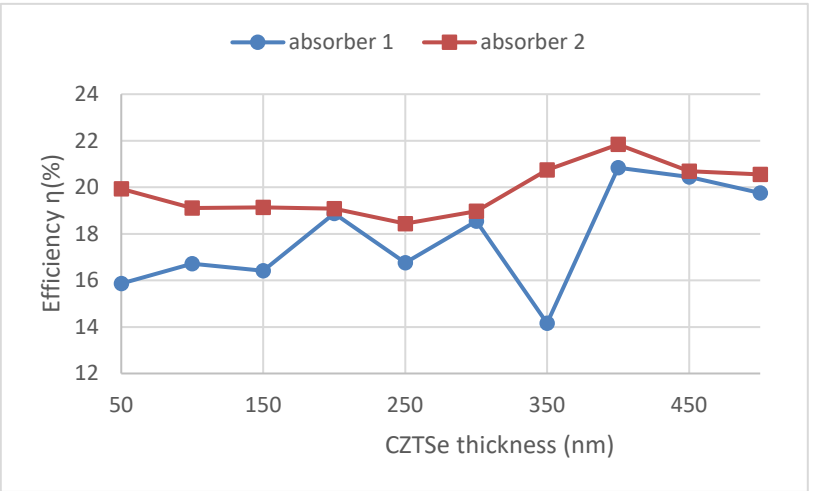

Figure 3: Effect of CZTSe thickness on the solar cell efficiency for both absorbers

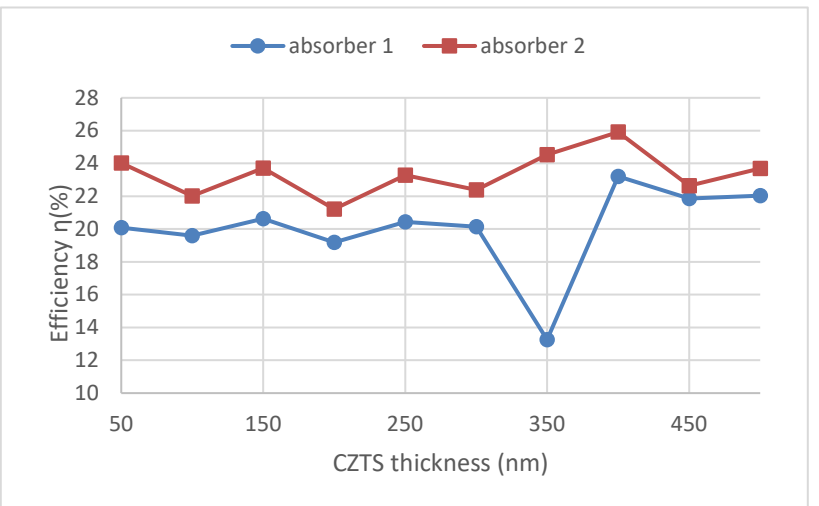

Figure 4: Effect of CZTS thickness on the solar cell efficiency for both absorbers

As previously stated, the absorber 2 consistently demonstrates higher values of V_{OC}, J_{SC}, FF and $\eta(\%)$ compared to absorber 1 across all studies. Thus, we are only presenting the efficiency $\eta(\%)$ output parameter. One can notice from figure, that a CZTSe thickness of 400 nm is found to be the optimal thickness for both absorber 1 and absorber 2, resulting in the highest efficiency of 20.84% and 21.84%, respectively. At this thickness, absorber 2 demonstrates higher efficiency than absorber 1.

From figure 4, a CZTS thickness of 400 nm is found to be the optimal thickness for both absorber 1 and absorber 2, resulting in the highest efficiency of 23.21% and 25.91%, respectively. Absorber 2 outperforms absorber 1 in terms of efficiency at this thickness.

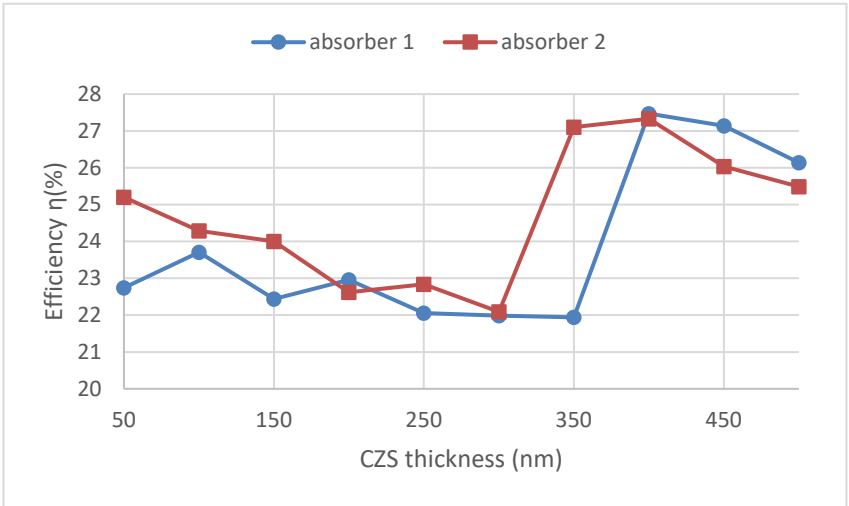

Figure 5: Effect of CZS thickness on the solar cell efficiency for both absorbers

From figure 5, a CZS thickness of 400 nm is found to be the optimal thickness for both absorber 1 and absorber 2, resulting in the highest efficiency of 27.47% and 27.33%, respectively. We can notice that both absorbers exhibit nearly identical maximum efficiency values at this particular thickness.

The table 1 exhibits the peak values of the solar cell output parameters for both absorbers 1 and 2 achieved with a buffer layer thickness of 400 nm.

Table 1: Highest solar cell output parameters achieved for different buffer layers

Buffer layer	$J_{SC}(mA/cm^2)$		$V_{OC}(V)$	
	Abs1	Abs2	Abs1	Abs2
CSTSe (400 nm)	24.3	27.8	1.06	0.959
CZTS (400 nm)	27.2	32.9	1.063	0.965
CZS (400 nm)	31.8	35.4	1.076	0.968
	$J_{SC}(mA/cm^2)$		$V_{OC}(V)$	
Without (600 nm)	Abs1	Abs2	Abs1	Abs2
	26.4	33.9	1.04	0.96

Table 1 (cont.): Highest solar cell output parameters achieved for different buffer layers

Buffer layer	$FF(\%)$		$\eta(\%)$	
	Abs1	Abs2	Abs1	Abs2
CSTSe (400 nm)	80.7	81.7	20.84	21.84
CZTS (400 nm)	80	81.3	23.21	25.91
CZS (400 nm)	79.9	79.6	27.47	27.33
	$FF(\%)$		$\eta(\%)$	
Without (600 nm)	Abs1	Abs2	Abs1	Abs2
	80	78	22.27	25.25

Figure 6 illustrates the power conversion efficiency of solar cells using absorbers 1 and 2, across various buffer layer thicknesses and types.

Previously mentioned, the optimal structural parameters were established to achieve maximum efficiency prior to the inclusion of the buffer layer. Consequently, comparing the output parameters of the solar cell for both absorbers 1 and 2 before and after the buffer layer is incorporated would lead to a clear understanding of the impact of the buffer layer. This would allow for the selection of the best absorber as well as the most suitable buffer layer.

Based on the results presented above, one can notice that the optimum buffer layer thickness obtained is 400 nm for the different buffer layers used. Absorber 2 is showing a highest efficiency value for CZTS and CZTSe buffer layers compared to absorber 1. However, it is showing a similar efficiency as absorber 1 for CZS buffer layer. Using these findings, a graph pointing out the efficiency of all studied buffer layers in term of layer thickness for both absorbers 1 and is given figure 15. This graph shows well the impact of the buffer layer implementation on the solar cell efficiency. Comparing to the solar cell efficiency without adding the buffer layer, a 400 nm optimum thickness of CZS buffer layer showed an increase in efficiency of 23.35% for absorber 1 and of 6.8% for absorber 2. A 400 nm optimum thickness of CZTS buffer layer showed an increase in efficiency of 4.22% for absorber 1 and of 1.3% for absorber 2. However, a 400 nm optimum thickness of CZTSe buffer layer showed a decrease in efficiency of 6.42% for absorber 1 and of 14.62% for absorber 2. Thus, when compared to CZTS and CZTSe, CZS emerges as the most favorable material option for the buffer layer, resulting in a maximum efficiency of 27% for absorbers 1 and 2. CZTS can also serve as a buffer layer for both absorbers 1 and 2, although with less improvement in efficiency. On the other hand, CZTSe does not provide a viable option for a buffer layer material for either absorber 1 or 2.

These results are proof on the importance of the buffer layer material choice in improving the solar cell efficiency.

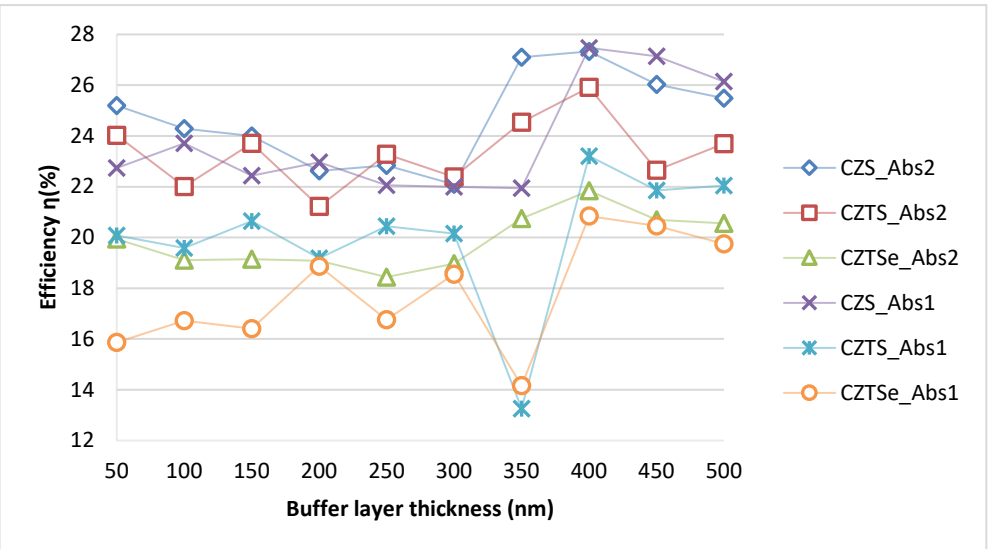

Figure 6: Effect of buffer layer thickness on the solar cell efficiency for both absorbers

5. CONCLUSION

The research conducted in this study employed the use of OghmaNano, a simulation tool that is instrumental in the development and optimization of photovoltaic devices, thereby advancing the technology and enhancing the efficiency and performance of solar cells. The solar cell structure was presented with its optimal material parameters, resulting in maximum performance and power conversion efficiency. Two types of absorbers, lead halide $MAPBCl_3$ (absorber 1) and lead-free $MAGeI_3$ (absorber 2), were investigated to determine which would provide the highest efficiency. An optimum thickness of 600 nm is found to produce the highest efficiency for both absorbers, with absorber 2 displaying superior efficiency to absorber 1 in the absence of a buffer layer.

The research also investigated the impact of buffer layer incorporation on solar cell efficiency. Three types of buffer layers, CSTSe, CSTS, and CZS, were applied to both absorbers 1 and 2, and optimized to achieve maximum efficiency in the PSC device structure. A thickness of 400 nm was found to produce the highest efficiency for all buffer layers and both absorbers. Absorber 2 displayed higher efficiency values with CZTS and CZTSe buffer layers compared to absorber 1 but had similar efficiency as absorber 1 with a CZS buffer layer. Compared to the solar cell efficiency without a buffer layer, an optimum thickness of 400 nm for a CZS buffer layer showed an increase in efficiency of 23.35% for absorber 1 and 6.8% for absorber 2. Meanwhile, an optimum thickness of 400 nm for a CZTS buffer layer resulted in an efficiency increase of 4.22% for absorber 1 and 1.3% for absorber 2. However, an optimum thickness of 400 nm for a CZTSe buffer layer resulted in a decrease in efficiency of 6.42% for absorber 1 and 14.62% for absorber 2. Ultimately, CZS emerged as the most favorable material option for the buffer layer, resulting in a maximum efficiency of 27% for both absorbers 1 and 2.

REFERENCES

[1] Kojima, A., Teshima, K., Shirai, Y., & Miyasaka, T. (2009). Organometal halide perovskites as visible-light sensitizers for photovoltaic cells. Journal of the american chemical society, 131(17)

[2] National Renewable Energy Laboratory (NREL). (2019). Best research-cell efficiencies. https://www.nrel.gov/pv/assets/pdfs/best-research-cell-efficiencies.pdf

[3] Umari, P., Mosconi, E., & De Angelis, F. (2014). Relativistic GW calculations on CH3NH3PbI3 and CH3NH3SnI3 perovskites for solar cell applications. Scientific Reports, 4(1), 4467.

[4] Yin, W.-J., Yang, J.-H., Kang, J., Yan, Y., & Wei, S.-H. (2015). Halide perovskite materials for solar cells: A theoretical review. Journal of Materials Chemistry A, 3(20), 8926-8942.

[5] Stranks, S. D., Snaith, H. J., Gracia-Espino, E., Leijtens, T., Mellor, C. J., LeLong, R., ... & Giustino, F. (2013). Electron-hole diffusion lengths exceeding 1 micrometer in an organometal trihalide perovskite absorber. Science, 342(6156), 341-344.

[6] Jin, H., Chen, J., & Snaith, H. J. (2020). It's a trap! On the nature of localized states and charge trapping in lead halide perovskites. Materials Horizons, 7(2), 397-410.

[7] Giustino, F., & Snaith, H. J. (2016). Toward lead-free perovskite solar cells. ACS Energy Letters, 1(6), 1233-1240.

[8] Ohara, K., Yamada, T., Tahara, H., Aharen, T., Hirori, H., Suzuura, H., & Kanemitsu, Y. (2019). Excitonic enhancement of optical nonlinearities in perovskite CH3NH3PbCl3 single crystals Phys. Rev. Materials, 3(11), 111601(R).

[9] Saparov, B., & Mitzi, D. B. (2016). Organic–Inorganic Perovskites: Structural Versatility for Functional Materials Design. Chemical Reviews, 116(7), 4558-4596.

[10] Stoumpos, C. C., Frazer, L., Clark, D. J., Kim, Y. S., Rhim, S. H., Freeman, A. J., ... Kanatzidis, M. G. (2015). Hybrid germanium iodide perovskite semiconductors: Active lone pairs, structural distortions, direct and indirect energy gaps, and strong nonlinear optical properties. Journal of the American Chemical Society, 137(17), 6804-6819.

[11] Krishnamoorthy, T., Ding, H., Yan, C., Leong, W. L., Baikie, T., Zhang, Z., ... Mhaisalkar, S. G. (2015). Lead-free germanium iodide perovskite materials for photovoltaic applications. Journal of Materials Chemistry A, 3(47),

[12] Nogay, G., Sahli, F., Werner, J., Monnard, R., Boccard, M., Despeisse, M., ... Ballif, C. (2019). 25.1%-Efficient monolithic perovskite/silicon tandem solar cell based on a p-type monocrystalline textured silicon wafer and high-temperature passivating contacts. ACS Energy Letters, 4(4), 844-845.

[13] Kanoun, A. A., Kanoun, M. B., Merad, A. E., & Goumri-Said, S. (2019). Toward development of high-performance perovskite solar cells based on CH3NH3GeI3 using computational approach. Solar Energy, 182, 237-244.

[14] Singh, R., Aluicio-Sarduy, E., Kan, Z., Ye, T., MacKenzie, R. C. I., & Keivanidis, P. E. (2014). Fullerene-free organic solar cells with an efficiency of 3.7% based on a low-cost geometrically planar perylene diimide monomer. Journal of Materials Chemistry A, 2(35), 14348-14353.

[15] Sims, L., Hörmann, U., Hanfland, R., MacKenzie, R. C., Kogler, F. R., Steim, R., ... & Schilinsky, P. (2014). Investigation of the s-shape caused by the hole selective layer in bulk heterojunction solar cells. Organic Electronics, 15(11), 2862-2867.

[16] Gao, Y., MacKenzie, R. C., Liu, Y., Xu, B., Van Loosdrecht, P. H., & Tian, W. (2015). Engineering ultra long charge carrier lifetimes in organic electronic devices at room temperature. Advanced Materials Interfaces, 2(4), 1400555.

[17] Le Corre, V. M., et al. (2019). Charge transport layers limiting the efficiency of perovskite solar cells: How to optimize conductivity, doping, and thickness. ACS Applied Energy Materials, 2(9), 6280-6287.

[18] Sha, W. E., Zhang, H., Wang, Z. S., Zhu, H. L., Ren, X., Lin, F., ... & Choy, W. C. (2018). Quantifying efficiency loss of perovskite solar cells by a modified detailed balance model. Advanced energy materials, 8(8), 1701586.

[19] Cai, B., Yang, X., Jiang, X., Yu, Z., Hagfeldt, A., & Sun, L. (2019). Boosting the power conversion efficiency of perovskite solar cells to 17.7% with an indolo[3{,}2-b]carbazole dopant-free hole transporting material by improving its spatial configuration. Journal of Materials Chemistry A, 7(24), 14835-14841.

[20] Peng, S. H., Huang, T. W., Gollavelli, G., & Hsu, C. S. (2017). Thiophene and diketopyrrolopyrrole based conjugated polymers as efficient alternatives to spiro-OMeTAD in perovskite solar cells as hole transporting layers. Journal of Materials Chemistry C, 5(21), 5193-5198.

[21] Kanoun, A. A., Kanoun, M. B., Merad, A. E., & Goumri-Said, S. (2019). Toward development of high-performance perovskite solar cells based on CH3NH3GeI3 using computational approach. Solar Energy, 182, 237-244.

[22] Abdelaziz, S., Zekry, A., Shaker, A., & Abouelatta, M. (2020). Investigating the performance of formamidinium tin-based perovskite solar cell by SCAPS device simulation. Optical Materials, 101, 109738.

[23] Adhikari, K. R., Gurung, S., Bhattarai, B. K., & Soucase, B. M. (2016). Comparative study on MAPbI3 based solar cells using different electron transporting materials. physica status solidi (c), 13(1), 13-17.

[24] Filippetti, A., & Mattoni, A. (2014). Hybrid perovskites for photovoltaics: Insights from first principles. Physical Review B, 89(12), 125203.

[25] Hou, F., Su, Z., Jin, F., Yan, X., Wang, L., Zhao, H., ... & Li, W. (2015). Efficient and stable planar heterojunction perovskite solar cells with an MoO 3/PEDOT: PSS hole transporting layer. Nanoscale, 7(21), 9427-9432.

[26] Qiu, X., Cao, B., Yuan, S., Chen, X., Qiu, Z., Jiang, Y., ... & Kanatzidis, M. G. (2017). From unstable CsSnI3 to air-stable Cs2SnI6: A lead-free perovskite solar cell light absorber with bandgap of 1.48 eV and high absorption coefficient. Solar Energy Materials and Solar Cells, 159, 227-234.

[27] Liu, M., Qi, Y., Zhao, L., Chen, D., Zhou, Y., Zhou, H., ... & Li, F. (2018). Matrix metalloproteinase-14 induces epithelial-to-mesenchymal transition in synovial sarcoma. Human Pathology, 80, 201-209.

[28] Guo, Z., Manser, J. S., Wan, Y., Kamat, P. V., & Huang, L. (2015). Spatial and temporal imaging of long-range charge transport in perovskite thin films by ultrafast microscopy. Nature Communications, 6(1), 7471.

[29] Leijtens, X. (2013). A generic approach to InP-based photonic ICs. 2013 IEEE Photonics Conference, Bellevue, WA, USA, 1-2.

[30] Kim, K. B., Kim, M., Lee, H. C., Park, S. W., & Jeon, C. W. (2017). Copper indium gallium selenide (CIGS) solar cell devices on steel substrates coated with thick SiO2-based insulating material. Materials Research Bulletin, 85, 168-175.

[31] Kapadnis, R. S., Bansode, S. B., Supekar, A. T., Bhujbal, P. K., Kale, S. S., Jadkar, S. R., & Pathan, H. M. (2020). Cadmium telluride/cadmium sulfide thin films solar cells: a review. ES Energy & Environment, 10(2), 3-12.

[32] Yao, J., Chen, Q., Zhang, C., Zhang, Z. G., & Li, Y. (2022). Perylene-diimide-based cathode interlayer materials for high performance organic solar cells. SusMat, 2(3), 243-263.

[33] Yan, C., Barlow, S., Wang, Z., Yan, H., Jen, A. K. Y., Marder, S. R., & Zhan, X. (2018). Non-fullerene acceptors for organic solar cells. Nature Reviews Materials, 3(3), 1-19.

[34] Chen, D., Nakahara, A., Wei, D., Nordlund, D., & Russell, T. P. (2011). P3HT/PCBM bulk heterojunction organic photovoltaics: Correlating efficiency and morphology. Nano Letters, 11(2), 561-567.

[35] Xu, L., Zhou, P., Wu, Y.-H., Xu, J., Wu, Y., & Xu, X.-W. (2019). Insight into adaptation mechanisms of marine bacterioplankton from comparative genomic analysis of the genus Pseudohongiella. Deep Sea Research Part II: Topical Studies in Oceanography, 167, 62-69.

[36] Xiong, L., Guo, Y., Wen, J., Liu, H., Yang, G., Qin, P., & Fang, G. (2018). Review on the application of SnO2 in perovskite solar cells. Advanced Functional Materials, 28(35), 1802757.

[37] Jiang, Q., Zhang, X., & You, J. (2018). SnO2: a wonderful electron transport layer for perovskite solar cells. Small, 14(31), 1801154.

[38] Yang, G., Li, X., Zhao, B., Liu, C., Zhang, T., Li, Z., ... & Li, X. (2022). Embedding SnO2 thin shell protected Ag nanowires in SnO2 ETL to enhance the performance of perovskite solar cells. Langmuir, 38(21), 6752-6760.

[39] Xu, Z., Teo, S. H., Gao, L., Guo, Z., Kamata, Y., Hayase, S., & Ma, T. (2019). La-doped SnO2 as ETL for efficient planar-structure hybrid perovskite solar cells. Organic Electronics, 73, 62-68.

[40] Ali, N., Hussain, A., Ahmed, R., Wang, M. K., Zhao, C., Haq, B. U., & Fu, Y. Q. (2016). Advances in nanostructured thin film materials for solar cell applications. Renewable and Sustainable Energy Reviews, 59, 726-737.

[41] Grimm, A., Klenk, R., Klaer, J., Lauermann, I., Meeder, A., Voigt, S., & Neisser, A. (2009). CuInS2-based thin film solar cells with sputtered (Zn, Mg) O buffer. Thin Solid Films, 518(4), 1157-1159.

[42] Innocenti, M., Becucci, L., Bencistà, I., Carretti, E., Cinotti, S., Dei, L., ... & Foresti, M. L. (2013). Electrochemical growth of Cu–Zn sulfides. Journal of Electroanalytical Chemistry, 710, 17-21.

[43] Minbashi, M., Omrani, M. K., Memarian, N., & Kim, D. H. (2017). Comparison of theoretical and experimental results for band-gap-graded CZTSSe solar cell. Current Applied Physics, 17(10), 1238-1243.

[44] Pal, K., Singh, P., Bhaduri, A., & Thapa, K. B. (2019). Current challenges and future prospects for a highly efficient (> 20%) kesterite CZTS solar cell: A review. Solar Energy Materials and Solar Cells, 196, 138-156.

[45] Huang, J., Yang, Y., Xue, S., Yang, B., Liu, S., & Shen, J. (1997). Photoluminescence and electroluminescence of ZnS: Cu nanocrystals in polymeric networks. Applied Physics Letters, 70(18), 2335-2337.

[46] Diamond, A. M., Corbellini, L., Balasubramaniam, K. R., Chen, S., Wang, S., Matthews, T. S., ... & Ager, J. W. (2012). Copper-alloyed ZnS as ap-type transparent conducting material. physica status solidi (a), 209(11), 2101-2107.

[47] Uhuegbu, C. C., & Babatunde, E. B. (2010). Spectral analysis of copper zinc sulphide ternary thin film grown by solution growth technique. American Journal of Scientific and Industrial Research, 1(3), 397-400.

[48] Yang, K., Nakashima, Y., & Ichimura, M. (2011). Electrochemical deposition of CuxS and CuxZnyS thin films with p-type conduction and photosensitivity. Journal of The Electrochemical Society, 159(3), H250.

[49] Sreejith, M. S., Deepu, D. R., Kartha, C. S., Rajeevkumar, K., & Vijayakumar, K. P. (2014). Tuning the properties of sprayed CuZnS films for fabrication of solar cell. Applied physics letters, 105(20), 202107.

[50] Emegha, J., Olofinjana, B., Ukhurebor, K., Aigbe, U., Azi, S. & Eleruja, M. (2022). Effect of Deposition Temperature on the Properties of Copper-Zinc Sulphide Thin Films using Mixed Copper and Zinc Dithiocarbamate Precursors. Gazi University Journal of Science, 35 (4) , 1556-1570.